International Journal of Scientific Research & Engineering Trends
Volume 12, Issue 6, Nov-Dec-2026, ISSN (Online): 2395-566X

Comparative Structural and Thermal Finite Element Analysis of a Single-Cylinder IC Engine Piston Using Aluminium Alloy, SS316 and AlSi10Mg

Arpita Sunil Kale[1], Guide Dr. T. Y. Badgujar[2]
Department of Mechanical Engineering Late G. N. Sapkal College of Engineering
Anjaneri, Nashik, Maharashtra, India[1,2]

Abstract — The piston is one of the most heavily loaded components of an internal combustion (IC) engine, since it must withstand cyclic gas pressure, steep thermal gradients and high reciprocating speeds. This paper presents the design and finite element analysis (FEA) of a piston for a single-cylinder, four-stroke engine with a 50 mm bore and 49.5 mm stroke. A three-dimensional model containing a concave crown, three ring grooves, gudgeon-pin bosses, internal ribs and fillets was developed in Autodesk Fusion 360 and analysed in ANSYS Workbench. Static structural analysis under a peak gas pressure of 5 MPa and steady-state thermal analysis were carried out for three candidate materials: an aluminium alloy, AISI 316 stainless steel (SS316) and the additively manufacturable alloy AlSi10Mg. The equivalent stress was almost material independent (169.7–184.8 MPa), whereas SS316 reduced the maximum deformation from 0.224 mm (aluminium) to 0.085 mm and lowered the peak total heat flux from 254.6 to 39.2 W/mm2. A hand calculation based on strength of materials reproduced the FEA stress within 0.5% and the same material ranking, which validates the load path and boundary conditions of the model. The results show that SS316 gives the greatest stiffness and the lowest heat rejection through the crown, while the aluminium alloys retain the advantage of low mass; the trade-offs are discussed to guide material selection.

Keywords— IC engine piston, finite element analysis, ANSYS, thermal analysis, structural analysis, SS316, AlSi10Mg, material selection

I. INTRODUCTION

The internal combustion engine converts the chemical en-ergy of fuel into mechanical work, and the piston is the component that receives the gas force and transmits it to the crankshaft through the connecting rod. During every cycle the crown is exposed to combustion gases whose tempera-ture can exceed 2000◦C and whose pressure reaches several megapascals, while the ring belt must seal the cylinder and the skirt must guide the piston against side thrust [1]. Repeated heating and cooling produce thermal fatigue, crown cracking, ring-groove wear and loss of sealing, which increases oil con-sumption and can end in seizure [2]. Piston design therefore has to balance strength, thermal resistance, wear behaviour and, because the piston reciprocates, low mass.

Aluminium alloys dominate small and medium engines because of their low density and high thermal conductivity, but their strength falls at elevated temperature. Steel pistons carry higher pressures at the cost of weight, and titanium alloys are used where cost is secondary to strength-to-weight ratio [3], [4]. Modern engines add turbocharging, higher compression ratios and tighter emission rules, which push piston loads higher still. Experimental piston testing is expensive and slow, so computer-aided design (CAD) and finite element analysis (FEA) are now routinely used to locate critical stress zones and compare materials before a prototype is made [5], [6].

This paper reports the design and analysis of a piston for a single-cylinder four-stroke engine. The specific contributions are: (i) a detailed CAD model including crown, ring grooves, pin bosses, ribs and fillets; (ii) structural and steady-state thermal FEA of this model for an aluminium alloy, SS316 and AlSi10Mg under identical loading; and (iii) an independent hand calculation used to check the FEA results.

II. LITERATURE REVIEW

Structural analysis. Static structural studies apply the gas pressure to the crown and constrain the pin region. Tamrakar et al. and Prabhakar et al. report that the maximum von Mises stress occurs near the pin boss and ring grooves while the crown carries a lower, more uniform stress, and that deforma-tion stays within allowable limits [6], [7]. Sadiq et al. analysed diesel pistons and found that steel gives lower deformation than aluminium but is heavier, whereas aluminium conducts heat better [4]. Nallapu et al. combined thermal and pressure loads

© 2026 IJSRET

in ANSYS and again located the highest stress at the crown and ring-groove region [5].

Thermal analysis. Mohanavel et al. and Rehman et al. showed that the crown is the hottest region and that temper-ature falls towards the skirt, producing gradients that stress the ring grooves [8], [9]. Gustof et al. measured higher crown temperatures with increasing load in turbocharged diesel pis-tons and showed the benefit of oil cooling [10]. Carlucci et al. simulated high-speed engines and found that thermal expansion alters piston–cylinder clearance [11]. Ding et al. and Ojo et al. studied near-wall flame and thermal boundary-layer behaviour, which supplies the transient boundary conditions that thermal models require [12], [13].

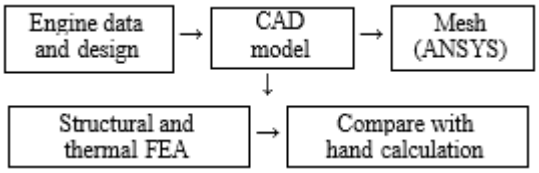


Fig. 1. Overall workflow adopted in this study.

Coupling, geometry and materials. Zhao et al. and Toledo Valera et al. concluded that fully coupled thermo-mechanical analysis is more accurate than separate thermal and structural runs [14], [15]. Rajesh et al. and Vijayan et al. showed that crown thickness, rib layout, fillets and bowl shape reduce stress concentration and mass [16], [17]. On materials, Babu et al. compared aluminium, cast iron, steel and titanium and recommended aluminium for general automotive use, steel for heavy-duty diesels and titanium for racing engines [3]; Rathore et al. reviewed composite pistons for weight reduction [18].

Research gap. Most studies treat thermal or structural be-haviour separately, often with simplified geometry, and few compare several materials under identical conditions for small single-cylinder engines. The present work addresses this by using a detailed piston geometry and a common set of loads for three materials, one of which (AlSi10Mg) is relevant to additive manufacturing.

III. METHODOLOGY

The work follows the sequence of Fig. 1: specification of engine data, calculation of piston dimensions, CAD mod-elling, import into ANSYS Workbench, meshing, structural and thermal solution for each material, and comparison with a theoretical estimate.

1. Engine Specification and Gas Load

The target is a four-stroke single-cylinder engine with a bore D = 50 mm, a stroke L = 49.5 mm and a compression ratio of 9.9:1 (Table II). The piston crown area and gas force follow from the bore and the peak cylinder pressure:

$$A = \frac{\pi}{} D^2 = 1963.5 \text{ mm}^2, F = pA. \quad (1)$$

The swept volume is $V_s = \frac{\pi}{4} D^2 L \approx 97.19 \text{ cm}^3$. For the peak pressure p = 5 MPa used in the structural analysis the resultant gas force is

$$F = 5 \times 1963.5 = 9817.5 \text{ N} \approx 9.82 \text{ kN}. \quad (2)$$

2. CAD Modelling

The piston was modelled in Autodesk Fusion 360 in four stages. (1) Half of the cross-section was sketched about the vertical axis with a radius of 24.75 mm, a length of 37 mm and a concave crown of 1.9 mm thickness, and was revolved to form the body. (2) Starting 5.6 mm below the top edge, rectangular cuts 2.01 mm deep and spaced 2.6 mm apart were patterned to form two compression-ring grooves and one oil-ring groove. (3) A 9 mm pin hole surrounded by a 14 mm boss was created on both sides of the skirt. (4) Internal ribs linking the crown underside to the pin bosses were added, all internal sharp edges were filleted to reduce stress concentration, and skirt relief was trimmed. The finished model is shown in Fig. 2(b); Fig. 2(a) identifies the standard piston terminology.

3. Materials

Three materials were compared (Table III). Aluminium alloy is the conventional choice owing to its low density and high conductivity. SS316 has the highest modulus and strength but a conductivity roughly ten times lower. AlSi10Mg is a cast/additively manufactured Al–Si alloy with properties close to aluminium but a lower conductivity. All materials were treated as linear elastic and isotropic.

4. Finite Element Model

The CAD model was imported into ANSYS Workbench (2021), assigned each material in turn, and meshed with an element size of 2.35 mm, fine span-angle centre and medium smoothing, giving 20,431 elements and 41,063 nodes (Fig. 2(c)). The same mesh, loads and constraints were used for all three materials so that differences in the results are due to the material alone.

Structural analysis: a uniform pressure of 5 MPa was ap-plied to the crown and fixed-support constraints were applied to

© 2026 IJSRET

represent the gudgeon-pin connection. The outputs were total deformation, equivalent elastic strain and equivalent (von Mises) stress.

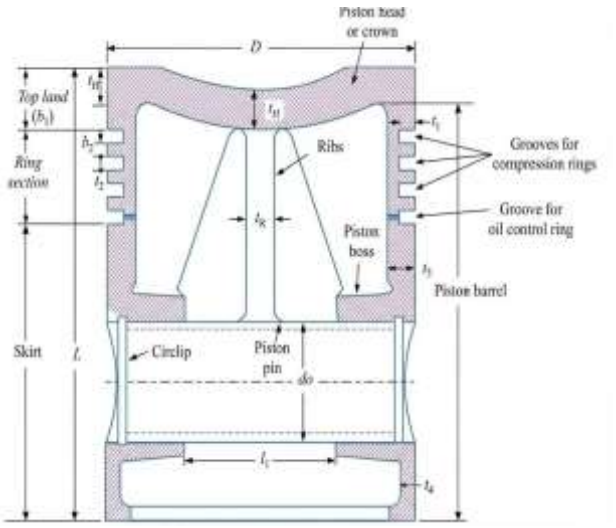
Steady-state thermal analysis: ambient temperature, sur-face temperature and convection boundary conditions were applied to the piston-head surfaces, and the total heat flux was recorded. A steady-state model gives a time-averaged picture suitable for comparing materials; it does not capture the cycle-to-cycle temperature swing. Heat transfer between a piston surface and the surrounding gas or oil follows Newton's law of cooling, q″ = h (T∞ − Ts), where h is the convective coefficient, T∞ the reference fluid temperature and Ts the local surface temperature; heat conduction inside the piston follows Fourier's law, $q'' = -k \nabla T$, so the conductivity k of each material directly controls the heat flux.

5. Theoretical Validation

To verify the FEA, the piston was idealised as an axial member of length Lp = 37 mm that transmits the gas force through an equivalent load-resisting area Aeff comprising the crown, ribs and pin bosses:

$$\sigma = \frac{F}{A_{\text{eff}}}, \qquad \varepsilon = \frac{\sigma}{E}, \qquad \delta = \varepsilon L_p. \tag{3}$$

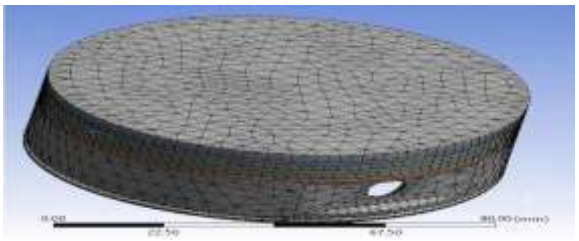
The values Aeff = 52.942, 56.585 and 57.614 mm2 were used for the aluminium alloy, SS316 and AlSi10Mg, respectively, and thermal effects were ignored in this check.



(a)



(b)



(c)

Fig. 2. (a) Piston terminology, (b) CAD model of the piston developed in Fusion 360, and (c) finite element mesh of the piston in ANSYS Workbench.

Table 2: Engine Specification and Piston Design Parameters

Engine parameter	Value	Piston parameter	mm
Type	4-stroke, 1 cyl.	Piston diameter	49.5
Bore	50 mm	Piston length	37
Stroke	49.5 mm	Crown thickness	1.9
Compression ratio	9.9:1	Pin hole diameter	9
Max. power at	8000 rpm	Pin boss outer diameter	14
Max. torque at	6000 rpm	Ring groove depth	2.01
Peak gas pressure	5 MPa	Gap between rings	2.6
		Top land thickness	5.6
		Ring radial thickness	2.0

Table 3: Mechanical and Thermal Properties of the Materials

Property	Al alloy	SS316	AlSi10Mg
Tensile strength (MPa)	395	550	317
Elastic modulus (GPa)	70	193	71
Poisson's ratio	0.33	0.29	0.33
Shear strength (MPa)	235	80.2	185
Fatigue strength (MPa)	125	270	124
Melting point (°C)	643	1400	596
Thermal conductivity (W/m·K)	170	16.3	113
Thermal diffusivity (mm^2/s)	71.63	4.38	43.78
Specific heat (J/kg·K)	879	500	963
Density (kg/m^3)	2700	7750	2600

© 2026 IJSRET

IV. RESULTS AND DISCUSSION

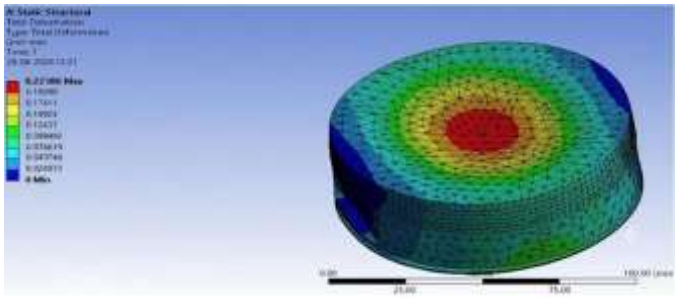
1. Structural Results

Fig. 3 shows representative ANSYS contours and Table IV summarises all results. For every material the largest deformation occurs at the centre of the thin concave crown, which bends under the 5 MPa gas pressure; deformation decreases towards the skirt and is zero at the constrained region. The aluminium alloy deforms by 0.22386 mm, AlSi10Mg by 0.20887 mm and SS316 by only 0.08469 mm, i.e. 62% less than the aluminium alloy. Equivalent strain follows the same order (0.00387, 0.00333 and 0.00124).

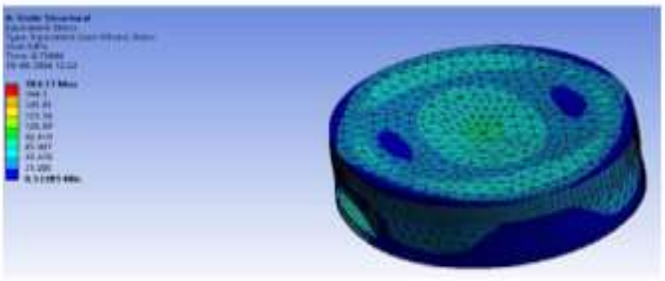
The equivalent stress, in contrast, varies little between materials: 184.77 MPa (aluminium alloy), 173.43 MPa (SS316) and 169.72 MPa (AlSi10Mg). This is expected because the load is a prescribed pressure, so the stress field is governed mainly by geometry and load path rather than by stiffness, whereas deformation scales approximately with 1/E. The ratio of the deformations of aluminium alloy and SS316 (2.64) is close to the ratio of their moduli (2.76), which supports the consistency of the model.

Table 4: Summary of Selected Literature on Piston Analysis

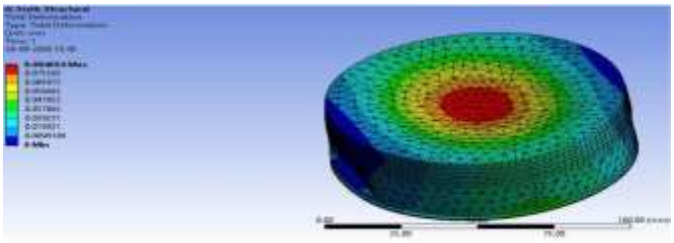
Reference	Focus	Method	Main finding
Tamrakar [6]	Structural analysis of Al piston	CAD + ANSYS FEM	Highest von Mises stress near pin boss and ring grooves; deformation within limits.
Prabhakar [7]	Static structural analysis	ANSYS Workbench	Fillets and smooth transitions reduce stress concentration; coupled analysis recommended.
Sadiq [4]	Diesel engine piston	ANSYS, material comparison	Steel gives lower deformation than aluminium but is heavier; aluminium conducts heat better.
Mohanavel [8]	Thermal analysis of Al piston	ANSYS thermal	Crown is hottest; ring grooves show elevated temperature and thermal-fatigue risk.
Gustof [10]	Effect of engine load	Experiment + numerical	Crown temperature rises with load; oil cooling lowers temperature and thermal stress.
Zhao [14]	Coupled thermo-mechanical model	Finite element	Coupled analysis is more accurate than separate thermal and structural runs.
Vijayan [17]	Crown shape modification	ANSYS (flat, bowl, dome)	Bowl crowns give lower thermal stress and better mixing than flat crowns.
Babu [3]	Piston material comparison	FEA, identical loads	Al lightest, steel stiffest, titanium best strength-to-weight but costly.



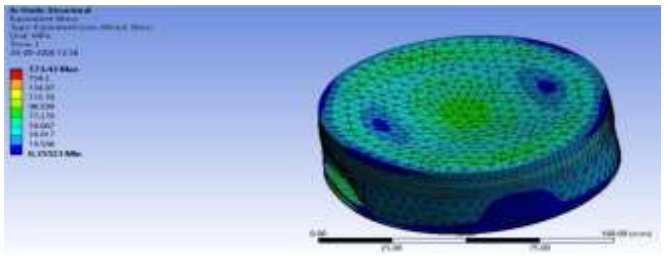
(a) Total deformation, Al alloy



(c) Equivalent stress, Al alloy

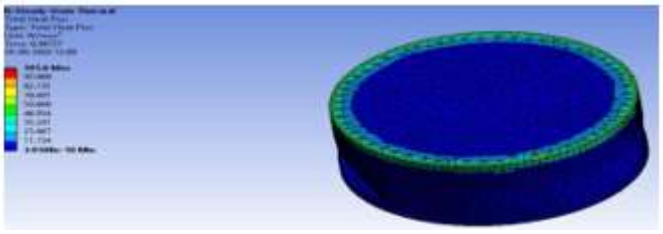


(b) Total deformation, SS316

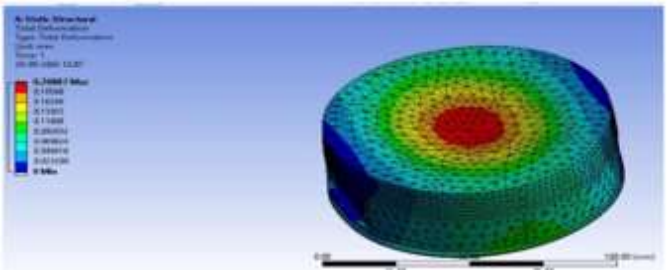


(d) Equivalent stress, SS316

© 2026 IJSRET



(e) Total heat flux, AlSi10Mg



(f) Total deformation, AlSi10Mg

Fig. 3. ANSYS contour plots of the piston. Deformation is in mm, stress in MPa and heat flux in W/mm2.

Table 4: Ansys Structural and Thermal Results and Static Safety

Material	Def. (mm)	Strain	Stress (MPa)	Heat flux (W/mm^2)	FoS[a]
Al alloy	0.22386	0.00387	184.77	254.64	2.14
SS316	0.08469	0.00124	173.43	39.20	3.17
AlSi10Mg	0.20887	0.00333	169.72	105.6	1.87

[a]Tensile strength divided by peak equivalent stress.

2. Thermal Results

The steady-state thermal results show a strong effect of conductivity. The peak total heat flux is 254.64 W/mm2 for the aluminium alloy, 105.6 W/mm2 for AlSi10Mg and 39.20 W/mm2 for SS316. The heat flux of SS316 is there-fore 85% lower than that of the aluminium alloy and 63% lower than that of AlSi10Mg, in line with its conductivity of 16.3 W/m·K compared with 170 and 113 W/m·K. In the contours the flux is concentrated along the crown periphery, which is the path by which heat leaves the crown towards the ring belt and cylinder wall (Fig. 3(e)). The values are used for comparison between materials; absolute metal temperatures would need calibrated gas-side heat-transfer coefficients and cooling data.

3. Comparison with the Theoretical Estimate

Table V compares the hand calculation with ANSYS. The stress agrees within 0.5% for all three materials, which con-firms that the pressure, loaded area and load path of the FE model are consistent with the analytical model. Strain and deformation from ANSYS are higher (by 38–46% and 128–155%, respectively), because the hand calculation assumes a uniform axial stress along the whole length, whereas the FE model includes the thin 1.9 mm crown, ribs, ring grooves, fillets and pin hole. Under pressure the crown bends, so local deformation and strain exceed the average values of the axial formula. Both methods give the same ranking—SS316 stiffest, aluminium alloy most flexible, AlSi10Mg close to the aluminium alloy—as illustrated in Fig. 4.

4. Material Suitability

Strength margin. Against the tensile strength the safety factors are 2.14 (aluminium alloy), 3.17 (SS316) and 1.87 (AlSi10Mg), so all three pass the static check, with SS316 having the largest margin. The fatigue strengths in Ta-ble III are, however, lower than the peak stress for the two aluminium-based materials (125 and 124 MPa against 184.8 and 169.7 MPa) but higher for SS316 (270 MPa against 173.4 MPa). Since a piston sees repeated loading, the static result should be followed by a fatigue assessment before the aluminium-based options are accepted for a 5 MPa duty.

Table 5: Comparison of Theoretical and Ansys Results

Material	Quantity	Theory	ANSYS	Diff. (%)
Al alloy	Deformation (mm)	0.09802	0.22386	+128.4
	Strain	0.002649	0.00387	+46.1
	Stress (MPa)	185.44	184.77	−0.4
SS316	Deformation (mm)	0.03326	0.08469	+154.6
	Strain	0.000899	0.00124	+37.9
	Stress (MPa)	173.50	173.43	−0.04
AlSi10Mg	Deformation (mm)	0.08880	0.20887	+135.2
	Strain	0.002400	0.00333	+38.8
	Stress (MPa)	170.40	169.72	−0.4

Stiffness and sealing. The low deformation of SS316 limits crown distortion and the associated loss of ring sealing and clearance, which is consistent with the lower deformation of steel pistons reported for diesel engines [3], [4].

Heat flow. The low heat flux of SS316 means less heat is conducted away through the crown, so more energy stays in the combustion chamber, which may help thermal efficiency. The same property will, however, raise the crown temperature, and the aluminium alloy's high conductivity remains an advantage for limiting thermal gradients and ring-groove temperature [9],

© 2026 IJSRET

[10]. A coupled thermo-mechanical analysis is needed to quantify this trade-off [14], [15].

Mass. The density of SS316 (7750 kg/m3) is 2.9 times that of the aluminium alloy (2700 kg/m3). For the same volume the reciprocating mass and inertia loads would rise accordingly, which is the main penalty of steel pistons and the reason aluminium dominates in high-speed engines [3], [16]. Mass reduction by thinner walls and optimised ribs would be required to benefit from steel.

Overall. On the basis of stiffness, strength margin and heat flux, SS316 is the best performer in this study and is a strong candidate for high-load applications. The aluminium alloy remains preferable where low mass and good heat dissipation govern, and AlSi10Mg offers an intermediate option with the possibility of additive manufacturing.

Applications and Limitations

Applications

The procedure used here, CAD modelling followed by structural and steady-state thermal FEA of several candidate materials, applies to any piston-type component. In two-wheeler and passenger-car engines it supports lightweight design for better fuel economy and acceleration, while for heavy-duty diesel, turbocharged and marine engines it helps to verify strength and crown deformation at high combustion pressure [4], [10]. Racing and high-performance engines, small auxiliary and generator engines, and future hydrogen or alternative-fuel engines, which run hotter, can use the same workflow to screen materials before manufacturing [3], [18]. It is also a useful teaching example of an end-to-end CAD–CAE workflow.

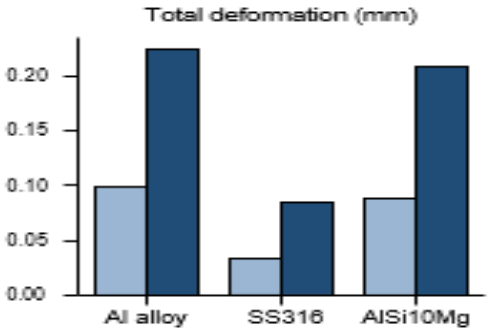
Limitations

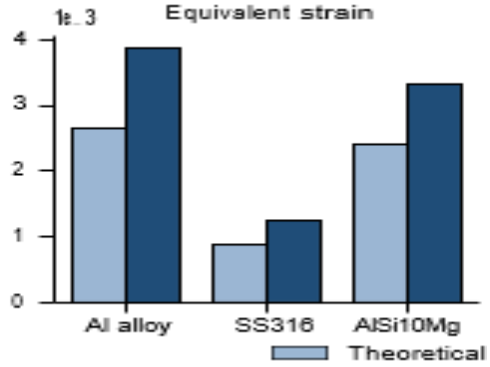
The results should be read within the following limits. (i) The peak pressure is applied as a static load, whereas the real pressure varies over the cycle, so cyclic fatigue life is not predicted. (ii) The thermal model is steady state and, in the structural solution, is not coupled with the thermal field; thermal stresses and the true crown temperature are therefore not obtained, although coupling is known to change the stress distribution [11], [14]. (iii) Inertia and side-thrust loads, lubrication and friction at the skirt, ring contact and manufacturing defects such as porosity are not modelled. (iv) The accuracy of any FE result depends on the assumed boundary conditions, mesh quality and material data, and experimental validation on an engine or test rig is still required.

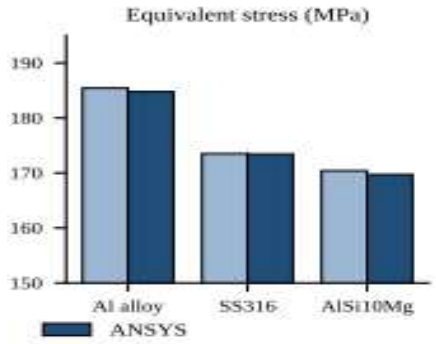
VII. CONCLUSION AND FUTURE SCOPE

A piston for a 50 mm bore, 49.5 mm stroke single-cylinder engine was modelled in Fusion 360 and analysed in ANSYS Workbench for an aluminium alloy, SS316 and AlSi10Mg. The main findings are:

The maximum equivalent stress was nearly the same for all materials (184.77, 173.43 and 169.72 MPa for the aluminium alloy, SS316 and AlSi10Mg), and was below the tensile strength of each material.







© 2026 IJSRET

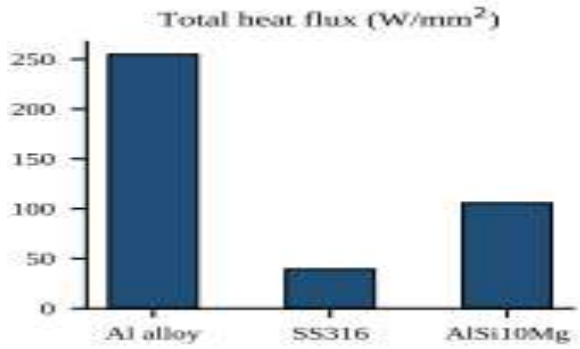


Fig. 4. Comparison of deformation, strain, stress and heat flux for the three materials. Theoretical values are available for the structural quantities only.

- SS316 gave the smallest deformation (0.08469 mm) and strain (0.00124), about 62% and 68% lower, re-spectively, than the aluminium alloy (0.22386 mm and 0.00387).
- SS316 gave the lowest peak total heat flux (39.20 W/mm2) against 254.64 and 105.6 W/mm2 for the aluminium alloy and AlSi10Mg.
- The hand calculation matched the FEA stress within 0.5% and reproduced the material ranking, validating the model; the larger FEA deformation arises from local crown bending that the axial model ignores.
- SS316 is the best choice for stiffness and strength margin, but its higher mass, lower conductivity and the lower fatigue strength of the aluminium materials must be considered in the final selection.

Future work should include coupled thermo-structural anal-ysis with calibrated gas-side heat-transfer coefficients and oil-cooling conditions, transient thermal loading, inertia and side-thrust loads, fatigue-life prediction, weight optimisation of the SS316 design, comparison with titanium alloy, and experimental validation.

Acknowledgment
The author thanks the project guide, Dr. T. Y. Badgujar, and Late G. N. Sapkal College of Engineering, Anjaneri, Nashik, for their guidance and support.

REFERENCES

1. R. Stone et al., Introduction to Internal Combustion Engine Component Design. New York, NY, USA: McGraw-Hill, 2015.
2. A. Bhutto et al., “Thermal effect on the automobile piston: A review,” Int. J. Sci. Eng. Res., vol. 7, no. 6, pp. 980–988, 2016.
3. V. Babu et al., “Comparative study of piston materials for IC engines,” Int. J. Adv. Eng. Res. Studies, vol. 1, no. 4, pp. 120–126, 2012.
4. S. Sadiq et al., “Finite element analysis of diesel engine pistons,” Int. J. Eng. Sci. Res. Technol., vol. 2, no. 9, pp. 2500–2507, 2013.
5. S. Nallapu et al., “Thermal and structural analysis of piston by ANSYS,” Int. J. Eng. Res. Technol., vol. 13, no. 2, pp. 78–85, 2024.
6. V. Tamrakar et al., “Structural analysis of IC engine piston using finite element method,” Int. J. Mech. Eng. Technol., vol. 9, no. 5, pp. 112–118, 2018.
7. K. Prabhakar et al., “Static structural analysis of IC engine pistons,” Int. J. Mech. Prod. Eng., vol. 2, no. 7, pp. 34–40, 2014.
8. V. Mohanavel et al., “Thermal analysis of IC engine piston using ANSYS,” Int. J. Eng. Res. Appl., vol. 8, no. 4, pp. 45–51, 2018.
9. A. Rehman et al., “Thermal stress analysis of aluminium pistons,” Int. J. Sci. Eng. Res., vol. 3, no. 5, pp. 1–6, 2012.
10. G. Gustof et al., “Influence of engine load on temperature distribution in turbocharged diesel engine pistons,” Appl. Therm. Eng., vol. 120, pp. 504–512, 2017.
11. P. Carlucci et al., “Numerical simulation of piston thermal behaviour in high-speed engines,” J. Therm. Sci. Eng. Appl., vol. 8, no. 3, pp. 1–10, 2016.
12. C.-P. Ding et al., “Flame/flow dynamics at the piston surface of an IC engine measured by high-speed PLIF and PTV,” Combust. Sci. Technol., vol. 192, no. 8, pp. 1450–1464, 2020.
13. A. O. Ojo et al., “Experimental investigation of thermal boundary layers and associated heat loss for transient engine-relevant processes,” Int. J. Heat Mass Transf., vol. 168, pp. 120–132, 2021.
14. F. Zhao et al., “Modeling and thermal-mechanical coupling analysis of piston in car engines,” J. Therm. Sci. Eng. Appl., vol. 9, no. 5, pp. 321–330, 2021.
15. J. D. Toledo Valera et al., “Thermal and structural improvements of a motorcycle piston using a fully coupled thermo-mechanical FEM simulation,” Int. J. Mech. Eng. Res., vol. 12, no. 3, pp. 145–156, 2025.
16. S. Rajesh et al., “Design optimization of aluminium alloy pistons,” Int. J. Innov. Res. Sci. Eng., vol. 3, no. 6, pp. 88–95, 2014.
17. P. Vijayan et al., “Design and structural analysis with thermal analysis of IC engine piston head with top surface

© 2026 IJSRET

modification," Int. J. Automot. Eng., vol. 10, no. 1, pp. 55–64, 2022.
18. P. S. Rathore et al., "A comprehensive review of stress and strain analysis in pistons utilizing composite materials via ANSYS software," J. Adv. Mech. Eng., vol. 11, no. 4, pp. 201–214, 2023.

© 2026 IJSRET